Journal of Electronic Materials (2024) 53:6090–6097
https://doi.org/10.1007/s11664-024-11377-2

ORIGINAL RESEARCH ARTICLE

Solution-Free Melt-Grown $CsGeI_3$ Polycrystals for Lead-Free Perovskite Photovoltaics: Synthesis, Characterization, and Theoretical Insights

Mariot Jose Panjikaran[1] · A. Pramitha[1] · Vikash Mishra[1] · Ganesh Shridhar Hegde[1,2] · Ashwatha Narayana Prabhu[1] · Nagabhushan Jnaneshwar Choudhari[1] · Abdelmajid Timoumi[3] · Y. Raviprakash[1]

Received: 24 April 2024 / Accepted: 7 August 2024 / Published online: 19 August 2024

Abstract

Inorganic lead-free metal halide perovskites are being rigorously explored as a substitute for organic lead-based materials for various energy device applications. Germanium as a replacement for lead has been proven to give exemplary results theoretically, and there have been promising results. The current work presents the investigation of $CsGeI_3$ (CGI) polycrystals grown using a solution-free melt-growth technique with low-cost precursors. A soak-ramp profile was designed to synthesize polycrystalline powders, which were evaluated for stability. X-ray diffraction and Raman spectroscopy analysis suggest the formation of $CsGeI_3$ perovskite powders, matching the reported literature. Diffuse reflectance spectroscopy measurements showed the bandgap of the polycrystals to be around 1.6 eV. A prominent photoluminescence peak was obtained at 767 nm. The powders were examined using thermogravimetric analysis to assess the thermal degradation pathways. The as-grown inorganic perovskite polycrystals were relatively stable during storage under ambient conditions. Theoretical studies were also carried out to support the experimental data. Calculations were performed with different approximations, including local density approximation (LDA), generalized gradient approximation (GGA), and Heyd–Scuseria–Ernzerhof (HSE) approximation, out of which the HSE approximation yielded the most accurate results that matched the experimental findings. Moreover, for the CGI device with Ag electrodes simulated using SCAPS-1D software, highest incident photon-to-electron conversion efficiency was observed. The obtained optical and structural properties indicate the suitability of the synthesized $CsGeI_3$ perovskite polycrystals for photovoltaic applications, specifically solar cells and light-emitting diodes.

Keywords Caesium germanium iodide · inorganic perovskites · lead-free perovskites · solar cells · photovoltaics · first-principles calculations

Introduction

Metal halide perovskite (MHP) materials have occupied the frontlines of optoelectronic research for over a decade, since 2009. Although the initial pioneering research on perovskites was entirely for photovoltaic (PV) applications, there has recently been a shift to exploration of other applications such as thermoelectric,[1,2] solar capacitors,[1] supercapacitors,[3,4] photoelectrochemical water splitting, photocatalysis,[5,6] photodetectors,[7–10] x-ray detectors,[11,12] and many more.[13–15] Considering PV application, MHPs have realized groundbreaking progress in terms of efficiency, with an over sixfold leap from efficiency of 3.8% ($CH_3NH_3PbI_3$ perovskite) in 2009[16] to 25.6% in 2021 ($CH(NH_2)_2PbI_3$ perovskite).[17] However, MHPs face a notable disadvantage in terms of stable performance under ambient environmental conditions. One of the major causes for the degradation of perovskite solar cells (PSCs) is the presence of hygroscopic organic cations such as methyl ammonium (CH_3NH_3/MA) and formamidinium ($CH(NH_2)_2$/FA). Further, the presence of lead (Pb) in the composition makes them unsuitable for consideration as a green energy solution.[18–22]

Over the years, various plausible solutions have been suggested to realize stable, environmentally friendly PSCs with good efficiency.[23,24] Research has been taken in multiple

✉ Y. Raviprakash
raviprakash.y@manipal.edu

1 Department of Physics, Manipal Institute of Technology, Manipal Academy of Higher Education, Manipal, India

2 Department of Physics, School of Applied Sciences, Reva University, Bengaluru, India

3 Department of Physics, Faculty of Applied Science, Umm AL-Qura University, 21955 Mecca, Saudi Arabia

directions, with attempts to tailor the basic ABX_3 perovskite structure at the A, B, and X sites to achieve the desired properties.[25–27] In this regard, inorganic lead-free MHPs are being extensively pursued by researchers, as the materials possess stellar optoelectronic properties that can be tuned to achieve benchmark performance. The most popular alternatives for replacing Pb at the B site are germanium (Ge),[10,28–39] tin (Sn),[23,40–45] antimony (Sb),[46–49] bismuth (Bi),[50–52] indium (In),[53–55] titanium (Ti),[56–59] and tellurium (Te).[60–62] Among these, Ge-based perovskites have proven to provide better stability and promising optoelectronic properties.[10,28,29,35,37,63,64] However, one factor that limits further experimental exploration of germanium-based perovskites is the high cost of the necessary precursors, especially germanium iodide (GeI_2). Also, the currently reported methods for the synthesis of $CsGeI_3$ powders are solution-based,[29] which is difficult to process for bulk and facile production.

In this work, we present a novel route for the synthesis of $CsGeI_3$ (CGI) polycrystals using low-cost precursors from the available alternatives. Instead of using germanium iodide, we propose the use of pure germanium precursor separately along with pure iodine and cesium iodide precursors to obtain the necessary composition. This method of using germanium powders and iodine crystals separately is found to significantly reduce the precursor cost (with a rough estimate of the current market prices, 10 times lower cost) for the synthesis of germanium iodide-based perovskites. Also, the devised route is a solution-free technique, which is more facile, provides better crystallinity, and contributes to the enhanced stability of the synthesized polycrystals. Fortunately, compared to 3 days, there was very little degradation of the CGI polycrystals observed over 45 days. Further, the experimental results correlated closely with the simulation outcomes undertaken via density functional theory (DFT) studies. Additionally, theoretical studies were performed on the CGI device configuration using various electrode materials.

Experimental Procedure

Synthesis of $CsGeI_3$ (CGI) Polycrystals

Inorganic lead-free MHP crystals have been successfully synthesized using the melt-quenching technique. In the present work, CGI polycrystals were synthesized using the solid-state reaction technique. Ge metal pieces (Alfa Aesar, 99.999%) and CsI powder (Alfa Aesar, 99.999%) were ground together for 2 h using an agate mortar and pestle. The finely ground sample was transferred to a clean quartz ampoule and loaded into the crystal puller. Resublimed iodine (I_2, Merck, 99.8%) crystals were added to the mixture just before loading into the crystal puller because of the volatile nature of iodine. Initially, the temperature was increased to 150°C and maintained for 10 h, then increased to 925°C and maintained for 24 h to ensure mixing, further maintained at 700°C for 24 h for homogeneity, and eventually cooled to room temperature. The process flowchart is presented in Fig. 1. The melt-quenching technique described by Xiao et al.[61] for the preparation of Cs_2TeI_6 crystals was modified according to the source materials and melting point of the compounds.

Characterization of Synthesized $CsGeI_3$ (CGI) Polycrystals

The structural analysis of the synthesized CGI polycrystals was carried out using x-ray diffraction (XRD) with Cu Kα [λ = 1.5405 Å] radiation at 40 kV and 15 mA in the 2θ range of 20°–60° (Rigaku MiniFlex 600). Raman spectroscopy was performed at an excitation wavelength of 532 nm using a LabRAM HR (UV). The prepared polycrystals were ground into powder, and the photoluminescence (PL) emission was studied using a Jasco FP-8300 fluorescence spectrometer using a 450 W xenon lamp. Also, the reflectance spectra were obtained for the powdered samples using a Lambda 950 UV–visible–near-infrared (NIR) spectrophotometer equipped with an integrating sphere (PerkinElmer, Waltham, MA, USA). Thermogravimetric analysis (TGA) was performed using a PerkinElmer TGA 4000 to observe the behaviour of the powders under temperature exposure.

Theoretical Studies

Quantum Espresso (QE) code was used for all the density functional theory (DFT)-based calculations.[65] All calculations were performed with 3 × 3 × 2 supercells, for pure CGI structures, and a k-point grid of 7 × 7 × 3 was used for integrations over the Brillouin zone. We used various approximations including the local density approximation (LDA), generalized gradient approximation (GGA), and Heyd–Scuseria–Ernzerhof (HSE) for the calculations.[66] Seo et al.

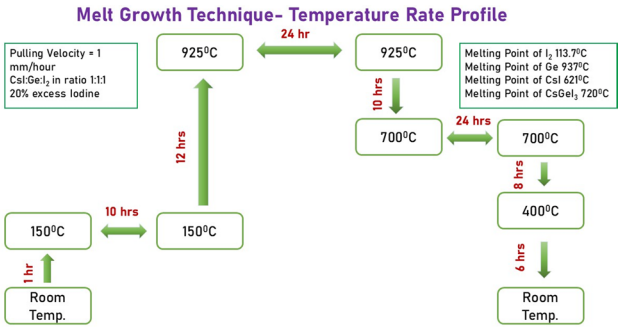

Fig. 1 Process flowchart.

showed that when using HSE to calculate the bandgaps of metal compounds which contain valence electrons in different orbitals, the mixing parameters must be optimized from typical values to see the variation in orbital overlapping.[67,68] Thus, to obtain a more accurate bandgap for $CsGeI_3$, the HSE calculation was used, with mixing parameters of 0.25 for all the calculations. Initially, we optimized the structures until the convergence of energy decreased to 5×10^{-5} eV and the value of force per atom reached 0.04 eV.[69] SCAPS-1D software was used to determine quantum efficiency measurements.[70]

Results and Discussion

Figure 2a shows the XRD diffractogram of the as-synthesized CGI polycrystals. The XRD pattern of the CGI crystals synthesized using the melt-quenching technique showed an excellent match with existing $CsGeI_3$ reports (JCPDS #01-085-1274).[64] The XRD pattern of the powdered ingot was acquired immediately after breaking the quartz ampoule and after an interval of 3 days to evaluate the sample's stability. The XRD pattern shows peaks corresponding to Ge and CsI, which could indicate possible decomposition of $CsGeI_3$ into its constituents CsI and Ge within just hours of exposure to an open environment. The XRD patterns obtained on day 3 further suggest the degradation of the sample, as shown in Fig. 2b. This agrees with the observations of Yue et al.[64] However, it is notable that even after 45 days of storage under ambient conditions, there is no further degradation observable for the CGI polycrystals. Also, such behaviour suggests the suitability of the synthesis route for employing solution-free solid-state methods to synthesize inorganic MHPs.

The Raman spectra shown in Fig. 3 agree with the reported data.[29] The strongest Raman peaks of the CGI crystal at 165 cm^{-1} can be attributed to the A_1 (longitudinal mode).[71] A minor peak detected at 337 cm^{-1} aligns with the overtone of CsI,[72] thereby confirming the existence of CsI, as indicated by XRD analysis. The low phonon frequencies observed in CGI suggest that its transparency range could be extended into the far-IR region.[73]

Further, diffuse reflectance spectroscopy (DRS) was performed, and the bandgap was found to be 1.6 eV, very close to previously reported values. Also, there was no change observed in the bandgap measured after 45 days. Kubelka–Munk theory was applied to estimate the bandgap from the reflectance spectra, with $n = 1/2$. The bandgap estimation from the plot is presented in Fig. 4. The estimated bandgap suggests the suitability of the synthesized CGI polycrystals for use in optoelectronic applications after being made into pellet or thin-film format, as has been previously reported.[10]

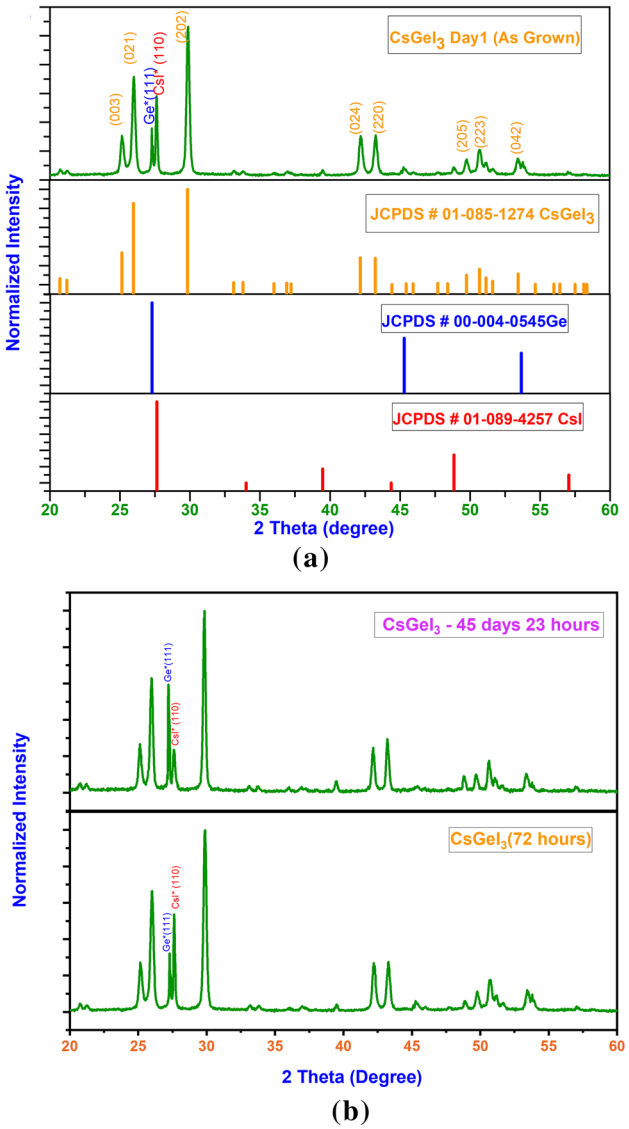

Fig. 2 (a) X-ray diffractogram of the as-synthesized CGI polycrystals. (b) Comparison of XRD patterns of CGI polycrystals: 3rd day and 45th day.

To match the experimentally obtained energy bandgap of $CsGeI_3$, theoretical studies were carried out. Accordingly, DFT calculations using QE code with different approximations were done to correlate with the DRS results. From Table I it is clear that out of all approximations, HSE calculation gives more accurate values of the electronic bandgap of CGI in comparison with the experimental outcome. The density of states is a crucial physical parameter for understanding the electronic properties of materials. Figure 5 shows the total density of states (TDOS) and partial density of states (PDOS) for $CsGeI_3$ simulated using the HSE approximation. It is clear that the highest energy level of the valence band in $CsGeI_3$ is primarily influenced by the halogen element iodine, while

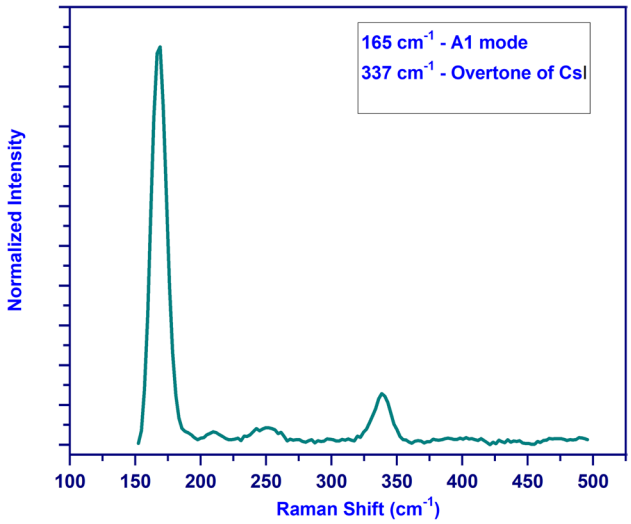

Fig. 3 Raman spectra of CGI polycrystals.

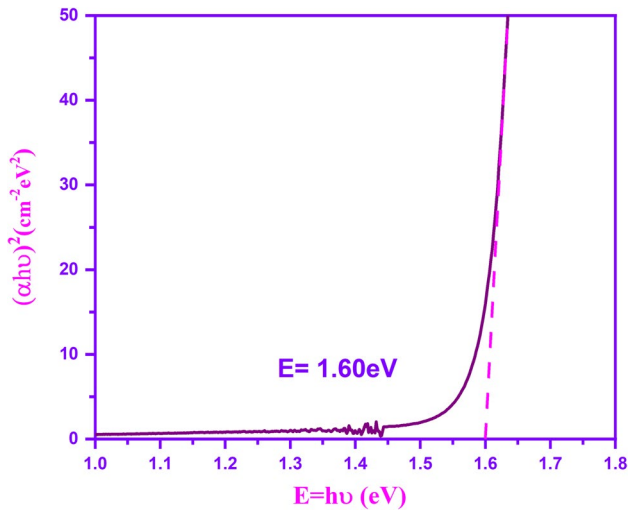

Fig. 4 Diffuse reflectance spectrum of the as-synthesized CGI polycrystals.

Table I Estimated electronic bandgaps of CGI using different approximations

Approximations	Electronic bandgap (eV)
LDA	0.80
GGA	1.10
HSE	1.58
Experimental	1.60

for the lowest occupied levels of the conduction band, Ge contributed the most.

The experimentally obtained $CsGeI_3$ polycrystals with the bandgap ranging between 1.5 and 1.6 eV (both theoretically and experimentally) have great potential for use in photovoltaics and photodetectors. In this direction, the device suitability of the $CsGeI_3$ polycrystals was checked theoretically with different type of electrodes. Systematic simulations were undertaken to investigate how different electrodes can have a notable impact on the performance of $CsGeI_3$ in photovoltaics and photodetection processes. Figure 6 depicts the simulation results of quantum efficiency studies. Figure 6a–c shows the circuit diagrams of the CGI device with different electrodes (Ag, Au, Pt). The estimated current density and incident photon-to-electron conversion efficiency (IPCE%) of the proposed devices clearly indicate the significant influence of different electrode materials on $CsGeI_3$ performance. It can be seen from Fig. 6d and e that the current density of CGI starts increasing with lower bias voltage in the case of the Au electrode, while the maximum IPCE% was observed for the Ag electrode. Moreover, the highest IPCE% was found to be independent of the electrodes and was seen at a wavelength of 760 nm.

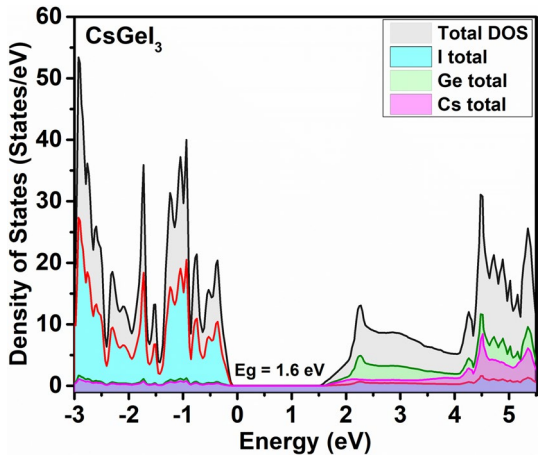

Fig. 5 Simulated total and partial density of states of $CsGeI_3$.

The photoluminescence studies conducted with an excitation wavelength of 660 nm reveal an intense broad peak centred around 798 nm and a peak of low intensity around 824 nm, as seen in Fig. 7. It can be observed that the emission at 798 nm corresponds to $E_g = 1.55$ eV, which is very close to the theoretical prediction (1.58 eV) as well as the experimentally observed (1.60 eV) bandgap. This high intense peak is attributed to electron transitions of the GeI_3 matrix and matches with reported data in the literature.[10] The peak around 824 nm is due to the perovskite matrix and observed for other inorganic MHPs as well.[74] Interband transitions in the perovskite matrix give rise to these emissions.[75]

The results of the thermogravimetric analysis of the as-prepared CGI powders are presented in Fig. 8. Transition temperatures of 415°C, 450°C, 500°C, 720°C, and 800°C were found for the respective compounds. TGA

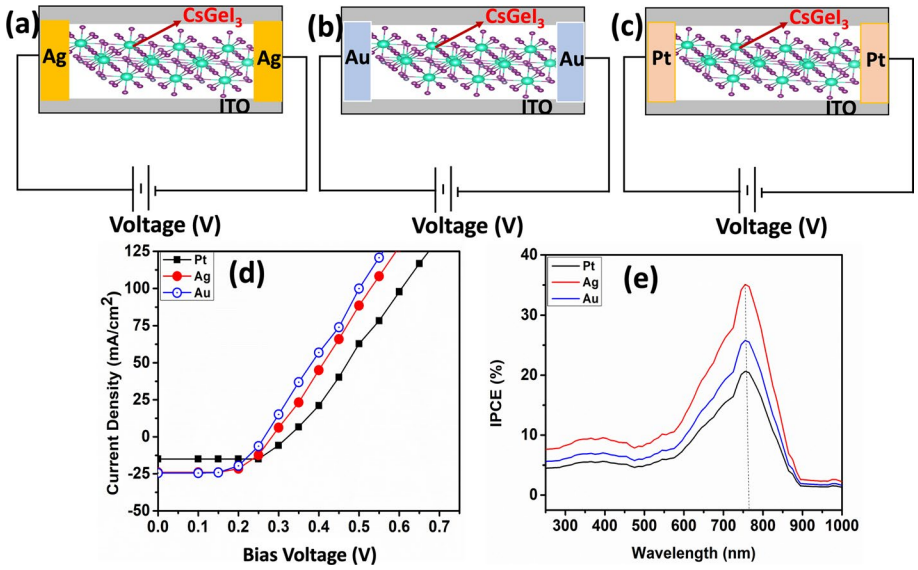

Fig. 6 (a–c) Schematic of the device structure of $CsGeI_3$ with (a) Ag, (b) Au, and (c) Pt electrodes. (d) Plot of current density vs bias voltage and (e) IPCE% vs wavelength with different electrodes.

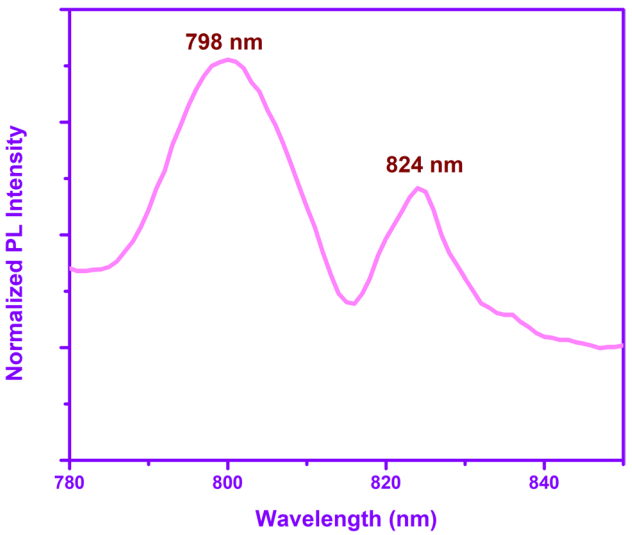

Fig. 7 Photoluminescence (PL) spectrum of the as-synthesized CGI polycrystals.

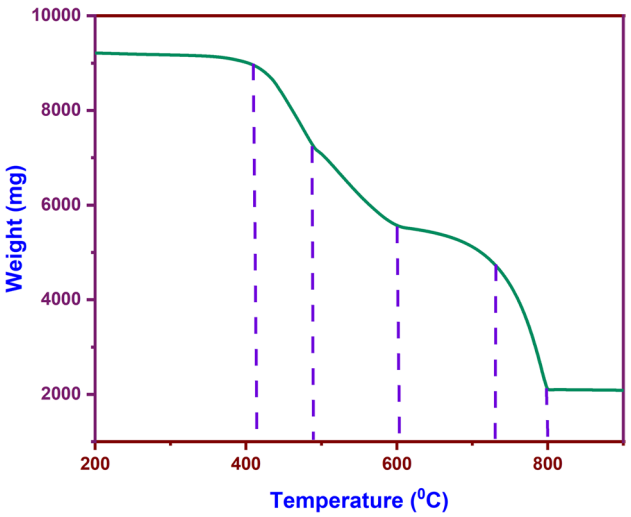

Fig. 8 Thermogravimetric analysis (TGA) curve of the as-synthesized CGI polycrystals.

was employed to investigate the decomposition of these perovskites under controlled, high-temperature conditions in air atmosphere from room temperature to 1000°C. The decomposition pathway under air atmosphere was accounted for by the apparent sharp weight loss observed. It was noted that the compound requires multiple steps for decomposition. The first stage is associated with the production of iodide molecules, escaping around 200–600°C. A subsequent steep weight loss in the second step is ascribable to the sublimation of GeI_2. At around 600°C, weight loss of about 50% of the initial weight is observed. The compound has a melting point of 790°C, which can also be seen from the TGA curves, which indicate complete disintegration around the same temperature.

Conclusions

In summary, $CsGeI_3$ (CGI) polycrystals were synthesized using the solution-free melt-growth technique, and their stability up to 45 days was investigated. X-ray diffraction and Raman studies confirmed the CGI structure with the appearance of some impurity phases because of the decomposition. After 3 days, there was slight degradation of the polycrystals. However, up until the 45th day, they remained largely steady in comparison to the third day. Further, optical

studies suggested that the bandgap of the synthesized powder was within the region of 1.6 eV. Also, a better correlation to the experimental results was achieved through DFT calculations with suitable approximation. The highest incident photon-to-electron conversion efficiency was observed for the CGI device with Ag electrodes. These $CsGeI_3$ powders can be further used for producing pellets or thin films. Moreover, the devised method can be applied to produce inorganic MHPs with enhanced stability. The experimental and theoretical outcomes suggest the suitability of the CGI for various optoelectronic applications. However, the observed decomposition of the polycrystals hinders its practical applicability. Strategies such as doping or halide cation composition optimization can be used to further increase the stability of these polycrystals by addressing structural defects, controlling ion migration, and optimizing the electronic properties of the material.

Acknowledgments The authors wish to acknowledge the Manipal Academy of Higher Education, Manipal, for providing all the support to carry out this research work. One of the authors (GSH) would like to thank REVA University for supporting this collaborative work.

Author contributions Mariot Jose Panjikaran: Conceptualization, Investigation, Formal analysis, Writing—original draft. Pramitha A: Formal analysis, Validation, Writing—review & editing. Vikash Mishra: Software, Validation, Writing—review & editing. Nagabhushan Jnaneshwar Choudhari: Validation, Writing—critical review & editing. Dr Ganesh Shridhar Hegde: Validation, Resources, Writing—review & editing. Dr Ashwatha Narayana Prabhu: Validation, Resources, Writing—review & editing. Abdelmajid Timoumi: Validation, Writing—review & editing. Dr Raviprakash Y: Conceptualization, Visualization, Validation, Writing—review & editing, Resources and Supervision.

Funding Open access funding provided by Manipal Academy of Higher Education, Manipal. The authors declare that no funds, grants, or other support were received during the preparation of this manuscript.

Data availability Data will be made available on request.

Competing interests The authors declare that they have no known competing financial interests or personal relationships that could have appeared to influence the work reported in this paper.

References

1. R. Liu, C. Liu, and S. Fan, A photocapacitor based on organometal halide perovskite and PANI/CNT composites integrated using a CNT bridge. *J. Mater. Chem. A* 5, 23078 (2017).
2. A.S.R. Bati, Y.L. Zhong, P.L. Burn, M.K. Nazeeruddin, P.E. Shaw, and M. Batmunkh, Next-generation applications for integrated perovskite solar cells. *Commun. Mater.* 4, 1 (2023).
3. S. Narayanan, N. Parikh, M.M. Tavakoli, M. Pandey, M. Kumar, A. Kalam, S. Trivedi, D. Prochowicz, and P. Yadav, Metal halide perovskites for energy storage applications. *Eur. J. Inorg. Chem.* 2021, 1201 (2021).
4. Y. Zhang, J. Chen, H. Dan, M. Maraj, B. Peng, and W. Sun, Energy storage and electrocaloric cooling performance of advanced dielectrics. *Molecules* 26, 26020481 (2021).
5. L. Romani, A. Speltini, C.N. Dibenedetto, A. Listorti, F. Ambrosio, E. Mosconi, A. Simbula, M. Saba, A. Profumo, P. Quadrelli, and F. De Angelis, Experimental strategy and mechanistic view to boost the photocatalytic activity of $Cs_3Bi_2Br_9$ lead-free perovskite derivative by g-C3N4 composite engineering. *Adv. Funct. Mater.* 31(46), 2104428 (2021).
6. X. Li, T. Zhang, T. Wang, and Y. Zhao, Recent progress of photocatalysis based on metal halide perovskites. *Acta Chim. Sin.* 77, 1075 (2019).
7. D. Luo, W. Yang, Z. Wang, A. Sadhanala, Q. Hu, R. Su, R. Shivanna, G.F. Trindade, J.F. Watts, Z. Xu, and T. Liu, Enhanced photovoltage for inverted planar heterojunction perovskite solar cells. *Science* 360(6396), 1442 (2018).
8. X. Zhou, L. Zhang, Y. Huang, Z. Zhou, W. Xing, J. Zhang, F. Zhou, D. Zhang, and F. Zhao, Enhanced responsivity of $CsCu2I_3$ based UV detector with cui buffer-layer grown by vacuum thermal evaporation. *Adv. Opt. Mater.* 9, 1 (2021).
9. R. Hany, M. Cremona, and K. Strassel, Recent advances with optical upconverters made from all-organic and hybrid materials. *Sci. Technol. Adv. Mater.* 20, 497 (2019).
10. H. Zeng, F. Yao, R. Li, D. Song, Y. Li, Q. Lin, and R.J. Xie, Thermal evaporation of lead-free inorganic perovskite $CsGeI_3$ for photodetection. *Appl. Phys. Lett.* 121, 108781 (2022).
11. H. Kim, J.S. Han, J. Choi, S.Y. Kim, and H.W. Jang, Halide perovskites for applications beyond photovoltaics. *Small Methods* 2, 1700310 (2018).
12. S. Zhao, W. Cai, H. Wang, Z. Zang, and J. Chen, All-inorganic lead-free perovskite(-Like) single crystals: synthesis. *Prop. Appl. Small Methods* 5, 1 (2021).
13. S. Il Seok and T.F. Guo, Halide perovskite materials and devices. *MRS Bull.* 45, 427 (2020).
14. L.M. Wheeler, D.T. Moore, R. Ihly, N.J. Stanton, E.M. Miller, R.C. Tenent, J.L. Blackburn, and N.R. Neale, Switchable photovoltaic windows enabled by reversible photothermal complex dissociation from methylammonium lead iodide. *Nat. Commun.* 8(1), 1722 (2017).
15. W. Zhang, G.E. Eperon, and H.J. Snaith, Metal halide perovskites for energy applications. *Nat. Energy* 1(6), 1–8 (2016).
16. K. Akihiro, K. Teshima, Y. Shirai, and T. Miyasaka, Organometal halide perovskites as visible-light sensitizers for photovoltaic cells. *J. Am. Chem. Soc.* 131, 6050 (2009).
17. J. Jeong, M. Kim, J. Seo, H. Lu, P. Ahlawat, A. Mishra, Y. Yang, M.A. Hope, F.T. Eickemeyer, M. Kim, Y.J. Yoon, I.W. Choi, B.P. Darwich, S.J. Choi, Y. Jo, J.H. Lee, B. Walker, Z.M. Shaik, L. Emsley, R. Ursula, A. Hagfeldt, D.S. Kim, M. Gratzel, and J.Y. Kim, Pseudo-halide anion engineering for α-$FAPbI_3$ perovskite solar cells. *Nature* 592, 381 (2021).
18. C.C. Zhang, S. Yuan, K.L. Wang, Z.K. Wang, and H. Okada, Improved photostability of metal halide perovskites by

microstructure modulation for photovoltaic application. *Org. Electron.* 101, 106380 (2022).
19. T. Miyasaka, A. Kulkarni, G.M. Kim, S. Öz, and A.K. Jena, Perovskite solar cells: can we go organic-free, lead-free, and dopant-free? *Adv. Energy Mater.* 10, 1 (2020).
20. Q. Fu, X. Tang, B. Huang, T. Hu, L. Tan, L. Chen, and Y. Chen, Recent progress on the long-term stability of perovskite solar cells. *Adv. Sci.* 5(5), 1700387 (2018).
21. C. Zhang, L. Gao, S. Hayase, and T. Ma, Current advancements in material research and techniques focusing on lead-free perovskite solar cells. *Chem. Lett.* 46, 1276 (2017).
22. N. Leupold and F. Panzer, Recent advances and perspectives on powder-based halide perovskite film processing. *Adv. Funct. Mater.* 31(14), 2007350 (2021).
23. M. Zhang, Z. Zhang, H. Cao, T. Zhang, H. Yu, J. Du, Y. Shen, X.L. Zhang, J. Zhu, P. Chen, and M. Wang, Recent progress in inorganic tin perovskite solar cells. *Mater. Today Energy* 1(23), 100891 (2022).
24. T. Xu, L. Chen, Z. Guo, and T. Ma, Strategic improvement of the long-term stability of perovskite materials and perovskite solar cells. *Phys. Chem. Chem. Phys.* 18, 27026 (2016).
25. S.T. Umedov, D.B. Khadka, M. Yanagida, A. Grigorieva, and Y. Shirai, A-site tailoring in the vacancy-ordered double perovskite semiconductor Cs_2SnI_6 for photovoltaic application. *Sol. Energy Mater. Sol. Cells* 230, 111180 (2021).
26. K. Xu, Development of tin-based perovskite materials for solar cell applications: a minireview. *Instrum. Sci. Technol.* 49, 91 (2021).
27. C. Wu, Y. Li, Z. Xia, C. Ji, Y. Tang, J. Zhang, C. Ma, and J. Gao, Enhancing photoluminescence of CsPb (ClxBr 1–x) 3 perovskite nanocrystals by Fe2+ doping. *Nanomaterials* 13(3), 533 (2023).
28. U.-G. Jong, Y.-S. Kim, C.-H. Ri, Y.-H. Kye, and C.-J. Yu, High thermoelectric performance in the cubic inorganic cesium iodide perovskites $CsBI_3$(B = Pb, Sn, and Ge) from first-principles. *J. Phys. Chem. C* 125, 6013 (2021).
29. R. Chen, C. Liu, Y. Chen, C. Ye, S. Chen, J. Cheng, S. Cao, S. Wang, A. Cui, Z. Hu, H. Lin, J. Wu, X.Y. Kong, and W. Ren, Ferroelectric $CsGeI_3$ single crystals with a perovskite structure grown from aqueous solution. *J. Phys. Chem. C* 127, 635 (2023).
30. X. Zhang, T. Li, C. Hu, Z. Fu, J. Lin, Z. Cheng, J. Wu, Y. Qi, Y. Ruan, and L. Huang, Investigation of efficient all-inorganic HTL-free $CsGeI_3$ perovskite solar cells by device simulation. *Mater. Today Commun.* 34, 105347 (2023).
31. X. Wu, W. Song, Q. Li, X. Zhao, D. He, and Z. Quan, Synthesis of lead-free $CsGeI_3$ perovskite colloidal nanocrystals and electron beam-induced transformations. *Chem. - An Asian J.* 13, 1654 (2018).
32. M.N. Islam, M.A. Hadi, and J. Podder, Influence of Ni doping in a lead-halide and a lead-free halide perovskites for optoelectronic applications. *AIP Adv.* 9(12), 125321 (2019).
33. K. A. Montiel, C. Yang, C. H. Andreasen, M. S. Gottlieb, M. R. Pfefferkorn, L. G. Wilson, J. L. W. Carter, and I. T. Martin, *Lead-Free Perovskite Thin Film Solar Cells from Binary Sources*, Conf. Rec. IEEE Photovolt. Spec. Conf. 1183 (2019).
34. T. Krishnamoorthy, H. Ding, C. Yan, W.L. Leong, T. Baikie, Z. Zhang, M. Sherburne, S. Li, M. Asta, N. Mathews, and S.G. Mhaisalkar, Lead-free germanium iodide perovskite materials for photovoltaic applications. *J. Mater. Chem. A* 3, 23829 (2015).
35. M. Azadinia, M. Ameri, R.T. Ghahrizjani, and M. Fathollahi, Maximizing the performance of single and multijunction ma and lead-free perovskite solar cell. *Mater. Today Energy J.* 4, 13852 (2021).
36. D. Liu, H. Peng, Q. Li, and R. Sa, A DFT study of the stability and optoelectronic properties of all-inorganic lead-free halide perovskites. *J. Phys. Chem. Solids* 161, 110413 (2022).
37. C.C. Stoumpos, L. Frazer, D.J. Clark, Y.S. Kim, S.H. Rhim, A.J. Freeman, J.B. Ketterson, J.I. Jang, and M.G. Kanatzidis, Hybrid germanium iodide perovskite semiconductors: active lone pairs, structural distortions, direct and indirect energy gaps, and strong nonlinear optical properties. *J. Am. Chem. Soc.* 137, 6804 (2015).
38. N. Chelil, M. Sahnoun, Z. Benhalima, R. Larbi, and S.M. Eldin, Insights into the relationship between ferroelectric and photovoltaic properties in $CsGeI_3$ for solar energy conversion. *RSC Adv.* 13, 1955 (2023).
39. N. Thi Han, V. Khuong Dien, and M.F. Lin, Electronic and optical properties of $CsGeX_3$ (X= Cl, Br, and I) compounds. *ACS Omega* 7(29), 25210 (2022).
40. A.K. Singh, S. Srivastava, A. Mahapatra, J.K. Baral, and B. Pradhan, Performance optimization of lead free-masni$_3$ based solar cell with 27% efficiency by numerical simulation. *Opt. Mater.* 1(117), 111193 (2021).
41. A.C. Dias, M.P. Lima, and J.L.F. Da Silva, Role of structural phases and octahedra distortions in the optoelectronic and excitonic properties of $CsGeX_3$(X = Cl, Br, I) perovskites. *J. Phys. Chem. C* 125, 19142 (2021).
42. J. Qian, B. Xu, and W. Tian, A comprehensive theoretical study of halide perovskites ABX_3. *Org. Electron.* 37, 61 (2016).
43. M. Roknuzzaman, K. Ostrikov, H. Wang, A. Du, and T. Tesfamichael, Towards lead-free perovskite photovoltaics and optoelectronics by ab-initio simulations. *Sci. Rep.* 7(1), 14025 (2017).
44. W. Ming, H. Shi, and M.-H. Du, Large dielectric constant, high acceptor density, and deep electron traps in perovskite solar cell material $CsGeI_3$. *J. Mater. Chem. A* 4, 13852 (2016).
45. C. Yu, Z. Chen, and K. Shum, Triply resonant raman scattering in perovskite semiconductor $CsSnI_3$. *J. Raman Spectrosc.* 44, 262 (2013).
46. K. Ahmad and S.M. Mobin, Recent progress and challenges in $A_3Sb_2X_9$-based perovskite solar cells. *ACS Omega* 5, 28404 (2020).
47. A. Singh, S. Najman, A. Mohapatra, Y.J. Lu, C. Hanmandlu, C.W. Pao, Y.F. Chen, C.S. Lai, and C.W. Chu, Modulating performance and stability of inorganic lead-free perovskite solar cells via lewis-pair mediation. *ACS Appl. Mater. Interfaces* 12, 32649 (2020).
48. S. Aina, B. Villacampa, and M. Bernechea, Earth-abundant non-toxic perovskite nanocrystals for solution processed solar cells. *Mater. Adv.* 2, 4140 (2021).
49. Y.N. Ivanov, A.A. Sukhovskii, V.V. Lisin, and I.P. Aleksandrova, Phase transitions of $Cs_3Sb_2I_9$, $Cs_3Bi_2I_9$, and $Cs_3Bi_2Br_9$ crystals. *Inorg. Mater.* 37, 623 (2001).
50. C. Teply, B.A. Tyler, and R.F. Berger, Tuning the band gaps of oxide and halide perovskite compounds via biaxial strain in all directions. *J. Phys. Chem. C* 125(47), 25951–25958 (2021).
51. P. Mariyappan, T.H. Chowdhury, S. Subashchandran, I. Bedja, H.M. Ghaithan, and A. Islam, Influence of Inorganic NiO_x hole transport layer on the growth of CsBi3I10 perovskite films for photovoltaic applications. *Adv. Mater. Interfaces* 8, 1 (2021).
52. T. Mohammad, V. Kumar, and V. Dutta, Effect of film thickness on the properties of bismuth iodide perovskite film for solar cell application. *AIP Conf. Proc.* 2115, 1 (2019).
53. A.D. Nicholas, R.N. Halli, L.C. Garman, and C.L. Cahill, Low-dimensional hybrid indium/antimony halide perovskites: supramolecular assembly and electronic properties. *J. Phys. Chem. C* 124, 25686 (2020).
54. J. Lin, K. Liu, H. Ruan, N. Sun, X. Chen, J. Zhao, Z. Guo, Q. Liu, and W. Yuan, Zero-dimensional lead-free halide with indirect optical gap and enhanced photoluminescence by Sb doping. *J. Phys. Chem. Lett.* 13, 198 (2022).
55. L. Zhou, J.F. Liao, Z.G. Huang, J.H. Wei, X.D. Wang, W.G. Li, H.Y. Chen, D.B. Kuang, and C.Y. Su, A highly red-emissive lead-free indium-based perovskite single crystal for sensitive water detection. *Angewandte Chem.* 131(16), 5331–5335 (2019).

56. M. Chen, M.G. Ju, A.D. Carl, Y. Zong, R.L. Grimm, J. Gu, X.C. Zeng, Y. Zhou, and N.P. Padture, Cesium titanium(IV) bromide thin films based stable lead-free perovskite solar cells. *Joule* 2, 558 (2018).
57. D. Kong, D. Cheng, X. Wang, K. Zhang, H. Wang, K. Liu, H. Li, X. Sheng, and L. Yin, Solution processed lead-free cesium titanium halide perovskites and their structural, thermal and optical characteristics. *J. Mater. Chem. C* 8, 1591 (2020).
58. P. Zhao, J. Su, Y. Guo, L. Wang, Z. Lin, Y. Hao, X. Ouyang, and J. Chang, Cs_2TiI_6: a potential lead-free all-inorganic perovskite material for ultrahigh-performance photovoltaic cells and alpha-particle detection. *Nano Res.* 15, 2697 (2022).
59. S. Ahmed, F. Jannat, M.A.K. Khan, and M.A. Alim, Numerical development of eco-friendly Cs_2TiBr_6 based perovskite solar cell with all-inorganic charge transport materials via SCAPS-1D. *Optik (Stuttg)* 225, 165765 (2021).
60. A.E. Maughan, A.M. Ganose, M.M. Bordelon, E.M. Miller, D.O. Scanlon, and J.R. Neilson, Defect tolerance to intolerance in the vacancy-ordered double perovskite semiconductors Cs_2SnI_6 and Cs_2TeI_6. *J. Am. Chem. Soc.* 138, 8453 (2016).
61. B. Xiao, F. Wang, M. Xu, X. Liu, Q. Sun, B.B. Zhang, W. Jie, P. Sellin, and Y. Xu, Melt-grown large-sized cs 2 tei 6 crystals for x-ray detection. *CrystEngComm* 22(31), 5130 (2020).
62. C.T. Li, M.X. Chong, L.X. Zhang, B. Tang, and L.J. Bie, All-inorganic lead-free halide perovskite Cs_2TeBr_6 enables real-time touchless human breath and finger related humidity monitoring. *Sens. Actuat. B Chem.* 379, 133240 (2023).
63. Y. Liu, Z. Xie, W. Zheng, P. Huang, Z. Gong, W. Zhang, Z. Shao, D. Yang, and X. Chen, High-efficiency narrow-band blue emission from lead-doped Cs_2ZnBr_4 nanocrystals. *Chem. Eng. J.* 460, 141683 (2023).
64. S. Yue, S.C. McGuire, H. Yan, Y.S. Chu, M. Cotlet, X. Tong, and S.S. Wong, Synthesis, characterization, and stability studies of ge-based perovskites of controllable mixed cation composition, produced with an ambient surfactant-free approach. *ACS Omega* 4, 18219 (2019).
65. P. Giannozzi, O. Andreussi, T. Brumme, O. Bunau, M.B. Nardelli, M. Calandra, R. Car, C. Cavazzoni, D. Ceresoli, M. Cococcioni, and N. Colonna, Advanced capabilities for materials modelling with quantum ESPRESSO. *J. Phys. Condens. Matter* 29(46), 465901 (2017).
66. V. Mishra, A. Sagdeo, V. Kumar, M.K. Warshi, H.M. Rai, S.K. Saxena, D.R. Roy, V. Mishra, R. Kumar, and P.R. Sagdeo, Electronic and optical properties of $BaTiO_3$ across tetragonal to cubic phase transition: an experimental and theoretical investigation. *J. Appl. Phys.* 122(6), 065105 (2017).
67. D.H. Seo, A. Urban, and G. Ceder, Calibrating transition-metal energy levels and oxygen bands in first-principles calculations: accurate prediction of redox potentials and charge transfer in lithium transition-metal oxides. *Phys. Rev. B* 92(11), 115118 (2015).
68. V. Mishra, M.K. Warshi, A. Sati, A. Kumar, V. Mishra, A. Sagdeo, R. Kumar, and P.R. Sagdeo, Diffuse reflectance spectroscopy: an effective tool to probe the defect states in wide band gap semiconducting materials. *Mater. Sci. Semicond. Process.* 86, 151 (2018).
69. A. Sumanth, V. Mishra, P. Pandey, M.S.R. Rao, and T. Dixit, Investigations into the role of native defects on photovoltaic and spintronic properties in copper oxide. *IEEE Trans. Nanotechnol.* 21, 522 (2022).
70. M. Burgelman, P. Nollet, and S. Degrave, Modelling polycrystalline semiconductor solar cells. *Thin Solid Films* 361, 527 (2000).
71. L.Y. Huang and W.R.L. Lambrecht, Vibrational spectra and nonlinear optical coefficients of rhombohedral $CsGeX_3$ halide compounds with X= I, Br, Cl. *Phys. Rev. B* 94, 1 (2016).
72. G.O. Amolo, R.M. Erasmus, J.D. Comins, and T.E. Derry, Raman and optical absorption studies of proton bombarded CsI. *Nucl. Instruments Methods Phys. Res. Section B: Beam Interact. Mater. Atoms* 250(1–2), 359–362 (2006).
73. G. Walters and E.H. Sargent, Electro-optic response in germanium halide perovskites. *J. Phys. Chem. Lett.* 9, 1018 (2018).
74. M. Chen, M.G. Ju, H.F. Garces, A.D. Carl, L.K. Ono, Z. Hawash, Y. Zhang, T. Shen, Y. Qi, R.L. Grimm, D. Pacific, X.C. Zeng, Y. Zhou, and N.P. Padture, Highly stable and efficient all-inorganic lead-free perovskite solar cells with native-oxide passivation. *Nat. Commun.* 10, 1 (2019).
75. L.C. Tang, C.S. Chang, and J.Y. Huang, Electronic structure and optical properties of rhombohedral $CsGeI_3$ crystal. *J. Phys. Condens. Matter* 12, 9129 (2000).